

Dominance of extrinsic scattering mechanisms in the orbital Hall effect: graphene, transition metal dichalcogenides and topological antiferromagnets

Hong Liu¹ and Dimitrie Culcer¹

¹*School of Physics and Australian Research Council Centre of Excellence in Low-Energy Electronics Technologies, UNSW Node, The University of New South Wales, Sydney 2052, Australia*

(Dated: August 30, 2023)

The theory of the orbital Hall effect (OHE), a transverse flow of orbital angular momentum in response to an electric field, has concentrated overwhelmingly on intrinsic mechanisms. Here, using a quantum kinetic formulation, we determine the full OHE in the presence of short-range disorder using 2D massive Dirac fermions as a prototype. We find that, in doped systems, extrinsic effects associated with the Fermi surface (skew scattering and side jump) provide $\approx 95\%$ of the OHE. This suggests that, at experimentally relevant transport densities, the OHE is primarily extrinsic.

Introduction. The electrical manipulation of magnetic degrees of freedom has been continuously investigated since Øersted discovered the deflection of a compass needle by a current-carrying wire. Modern research has focused on the magneto-electric coupling provided by the spin-orbit interaction [1–4], while an energetic recent effort has been geared towards the electrical operation of orbital degrees of freedom in systems without spin-orbit coupling [5–12]. This effort centers on the realization that Bloch electrons, despite being delocalized, possess an orbital angular momentum (OAM) about their center of mass [13], which is in part related to the Berry curvature [14–18]. The OAM affects semiclassical quantization [15, 17, 18], contributes to the magnetization in certain time-reversal breaking materials [19–21], affects the Zeeman splitting of Dirac materials [22, 23] and contributes to the non-linear magneto-resistance, valley-Hall effect [19, 24, 25], and anomalous Nernst effect [26].

In a time-reversal symmetric system, although there is no net OAM, a finite OAM density can be generated by an electric field. One way to generate an OAM is through the orbital Edelstein effect [27–31], which is, however, relatively restrictive. A more general method involves separating electrons with different OAMs on different sides of the sample using an electric current. This is the orbital Hall effect (OHE) [7, 10, 32–39], which has received considerable attention recently [11, 12, 20, 34, 40–43]. The OHE has been proposed as the mechanism behind the valley Hall effect observed in graphene and transition metal dichalcogenides (TMDs) [33, 44]. Injection of an orbital current into a ferromagnet using the OHE is expected to generate an orbital torque on local magnetic moments [11, 12, 20, 34, 40–43], and the OHE may likewise be responsible for the large spin Hall effect observed recently [10, 35–39]. Remarkably, all recent theoretical work has focused on intrinsic mechanism in the OHE [45–49], while neglecting the extrinsic disorder contribution. This absence is puzzling, since extrinsic scattering mechanisms such as skew scattering and side jump are known to contribute to the anomalous and spin-Hall effects at the same order in the disorder strength as the intrinsic contribution [37, 50–56], and it is natural to expect a substantial disorder contribution in the OHE as well.

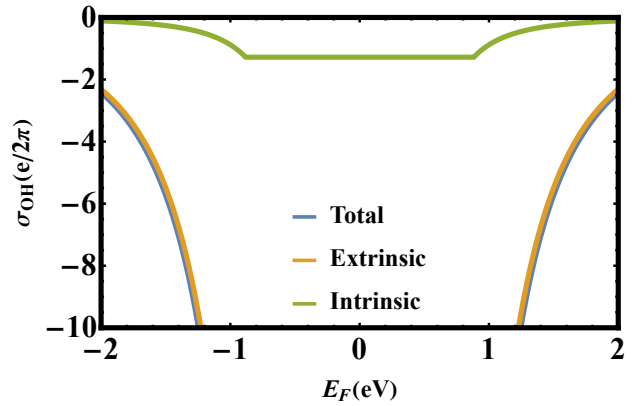


Figure 1. The total, extrinsic and intrinsic OH-conductance σ_{OH} vs the Fermi energy E_F for the 2H-phase monolayer MoS₂. One can see the dominance of the extrinsic contribution when E_F is not in the band gap. The parameters are $v_F = 3.6 \text{ eV}\text{\AA}$ and $2\Delta = 1.766 \text{ eV}$, and the intrinsic OHE is consistent with Ref. [46].

Unless their role is understood a meaningful comparison between theory and experiment cannot be performed.

In this article we calculate the full OHE, including intrinsic and extrinsic contributions, for 2D massive Dirac fermions, using graphene, TMDs, and topological antiferromagnets as prototype systems. In the latter case we do not incorporate corrections of second order in the ratio between the tilt and the Fermi velocity, which are expected to be negligible. The orbital current operator is defined as $\hat{\mathbf{j}} = \frac{1}{2}\{\hat{\mathbf{L}}, \hat{\mathbf{v}}\}$ where $\hat{\mathbf{L}}$ is the OAM operator and $\hat{\mathbf{v}}$ is velocity operator. We employ a quantum kinetic equation for the density matrix ρ , derived directly from the quantum Liouville equation, following the blueprint of Refs. [54, 57]. Our quantum mechanical formalism accounts for skew scattering and side jump effects, as well as the electric-field correction to the collision integral, which is vital in obtaining the correct result. In this language, skew scattering and side jump are contained in: (i) the inter-band part of the density matrix through the *anomalous driving term* of Ref. [54], and in (ii) the sub-leading correction to the intra-band part of

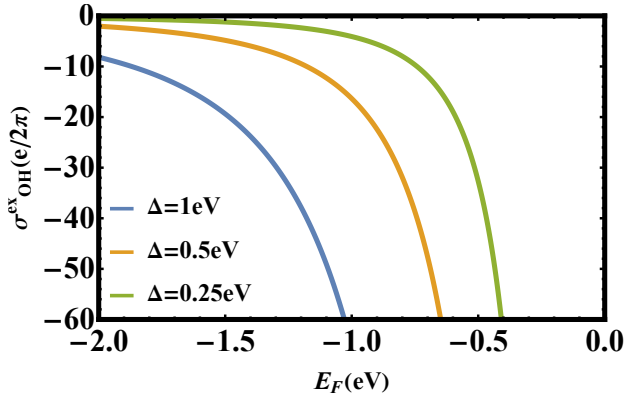


Figure 2. The extrinsic OH-conductance $\sigma_{\text{OH}}^{\text{ext}}$ vs the Fermi energy E_F for different energy band gaps. The parameters are taken from graphene $v_F = \frac{3}{2}at$ with $a = 1.42\text{\AA}$ and $t = 2.8\text{eV}$, and the intrinsic OHE is consistent with that of tight-binding model at large t^2/Δ regime [33].

the density matrix [57]. We find that the extrinsic OHE overwhelms the intrinsic contribution in doped systems and provides the dominant contribution to the orbital Hall current when the Fermi energy lies in the conduction or valence bands. For the model studied here of massive Dirac fermions, and assuming short-range impurities, the extrinsic contribution is 21 times of the intrinsic one. Our central result is summarized in Fig. 1, where we plot the total, intrinsic and extrinsic OH-conductance σ_{OH} vs Fermi energy separately. With the applied electric field E_x along the \hat{x} -direction, the orbital Hall current density for the z -component of the OAM, j_y^z , flows along the \hat{y} -direction. In this case $\sigma_{\text{OH}} = \sigma_{yx}^z = j_y^z/E_x$. The intrinsic OH-conductance is continuous and attains the maximum absolute value when the Fermi level is within the energy gap. As the Fermi level shifts on either side of the energy spectrum, both intrinsic and extrinsic OHE decrease. Based on the magnitude of extrinsic and intrinsic OH-conductance shown in Fig. 1, when the chemical potential lies either in the valence or in the conduction band the total OH-conductance essentially follows the extrinsic contribution. Physically, the dominance of extrinsic mechanisms reveals the strong role played by disorder-induced interband coherence in the transport of OAM. The OAM is an interband effect, and its intrinsic part is large in systems exhibiting large Berry curvatures, in other words strong intrinsic interband coherence. On the other hand skew scattering and side jump are sources of interband coherence mediated by disorder. Our calculation shows that, in the case of the OHE, this disorder-mediated contribution is one order of magnitude larger than the intrinsic terms, suggesting the best method to maximize the orbital Hall current may be to harness extrinsic mechanisms. Importantly, to obtain a large OHE it is *not* necessary for the Berry curvature to be large, a finding that has profound implications for the electrical manipulation of magnetic moments.

Main Results. With the external electrical field $\parallel \hat{x}$, and the total orbital Hall conductance $\sigma_{\text{OH}}^{\text{tot}} = \sigma_{yx}^z = -\sigma_{xy}^z$ when the Fermi energy lies in the valence or conduction band reads

$$\sigma_{\text{OH}}^{\text{tot}} \approx -\frac{g_s g_\nu}{4\pi} \frac{e m_e v_F^2}{3\hbar^2 \Delta} \frac{22\Delta^3}{(v_F^2 q_F^2 + \Delta^2)^{3/2}}, \quad (1)$$

where m_e is the electron mass, v_F is the Fermi velocity and 2Δ is the energy gap and g_s is the spin degeneracy and g_ν is valley degeneracy. The extrinsic contribution is $\sigma_{\text{OH}}^{\text{ext}} = \frac{21}{22}\sigma_{\text{OH}}^{\text{tot}}$ which is purely a Fermi surface effect and the intrinsic contribution is $\sigma_{\text{OH}}^{\text{int}} = \frac{1}{22}\sigma_{\text{OH}}^{\text{tot}}$ and is a Fermi sea effect. For Fermi energy is in the gap, only intrinsic contribution survives $\sigma_{\text{OH}}^{\text{int}} = -\frac{g_s g_\nu}{4\pi} \frac{e m_e v_F^2}{3\hbar^2 \Delta}$. For the bilayer, however, the height of the OHC plateau is essentially twice the monolayer value, while the SHC remains null in the main energy gap because it is topologically trivial [46]. The intrinsic and extrinsic contributions to the OHE have been plotted in Fig. 1 as a function of the Fermi energy for monolayer MoS₂, which reveals the dominance of the extrinsic OHE when the Fermi energy is away from the band gap. The intrinsic OHE is a continuous function of the Fermi energy E_F . The extrinsic OHE, on the other hand, is not continuous since it arises from the Fermi surface, and is necessarily zero in the gap.

Kinetic equation. We start with the quantum Liouville equation for the single particle density operator ρ ,

$$\frac{\partial \rho}{\partial t} + \frac{i}{\hbar} [H, \rho] = 0, \quad (2)$$

where the total Hamiltonian $H = H_0 + V(\mathbf{r}) + U(\mathbf{r})$. H_0 is the band Hamiltonian, $V(\mathbf{r}) = e\mathbf{E} \cdot \mathbf{r}$ is the external longitudinal electrical field, and $U(\mathbf{r})$ represents the disorder scattering potential, which we take to be scalar and short-range. We decompose the density matrix as $\rho = \langle \rho \rangle + g_0$, where $\langle \rho \rangle$ is averaged over disorder configurations, while g_0 is the fluctuating part [57]. EQ. (2) is decomposed into

$$\begin{aligned} \frac{\partial \langle \rho \rangle}{\partial t} + \frac{i}{\hbar} [H_0, \langle \rho \rangle] + J(\langle \rho \rangle) &= -\frac{i}{\hbar} [V, \langle \rho \rangle], \\ \frac{\partial g_0}{\partial t} + \frac{i}{\hbar} [H_0, g_0] &= -\frac{i}{\hbar} [U, \langle \rho \rangle] - \frac{i}{\hbar} [V, g_0]. \end{aligned} \quad (3)$$

In order to solve the kinetic equation for $\langle \rho \rangle$, we firstly solved the equilibrium and electrical field corrected fluctuating density matrix $g = g_0 + g_E$ where $g_0 = -\frac{i}{\hbar} \int_0^\infty dt' [e^{-iH_0 t'/\hbar} U e^{iH_0 t'/\hbar}, \langle \rho(t) \rangle]$ and $g_E = -\frac{i}{\hbar} \int_0^\infty dt'' e^{-iH_0 t''/\hbar} [V, g_0(t-t'')] e^{iH_0 t''/\hbar}$ [57]. Furthermore, fed g into the disorder averaged kinetic equation for $\langle \rho \rangle$, and we will get the kinetic equation

$$\frac{\partial \langle \rho \rangle}{\partial t} + \frac{i}{\hbar} [H_0, \langle \rho \rangle] + J_0(\langle \rho \rangle) = -\frac{i}{\hbar} [V, \langle \rho \rangle] - J_E(\langle \rho \rangle), \quad (4)$$

where the electrical field corrected scattering term $J_E(\langle \rho \rangle) = \frac{i}{\hbar} \langle [U, g_E] \rangle$ with g_E the correction to fluctuating part of density matrix [57] and the bare collision

integral $J_0(\langle \rho \rangle) = \frac{i}{\hbar} \langle [U, g_0] \rangle$. We take the same strategy to calculate the density matrix with disorder effect as that in Refs. [54, 57]. The disorder averaged density matrix $\langle \rho \rangle = \rho_0 + \rho_E$, where ρ_0 is the density matrix in equilibrium and $\rho_E = n_E + S_E$ is correction by external electrical field. The kinetic equation is solved in terms of band-diagonal contribution n_E and band off-diagonal contribution S_E . The band Hamiltonian of 2D Dirac material in a general form of H_0 , including the most experiment interested tunable parameters: Fermi velocity v_F , tilt v_t and energy gap 2Δ .

Graphene and TMDs. H_0 of monolayer graphene or TMDs has the form

$$H_0(\mathbf{q}) = v_F(\nu \tau_x q_x - \tau_y q_y) + \Delta \tau_z. \quad (5)$$

2Δ represents a gap that can be induced by inversion symmetry breaking, $\nu = \pm 1$ is the valley index for materials with valley degree, $\tau_{x,y,z}$ are the Pauli matrices: in graphene or TMDs these represent the sublattice pseudospin, and $\arctan \phi = q_y/q_x$. The band dispersion $E_{\mathbf{q}}^{\pm} = \pm E_q$ with $E_q = \sqrt{v_F^2 q^2 + \Delta^2}$. Take $\nu = 1$, the two eigenstates of band Hamiltonian are $|u_{+\mathbf{q}}\rangle = (u_q, v_q e^{-i\phi})^T$ and $|u_{-\mathbf{q}}\rangle = (v_q, -u_q e^{-i\phi})^T$ with $u_q = \sqrt{1/2(1 + \Delta/E_q)}$ and $v_q = \sqrt{1/2(1 - \Delta/E_q)}$. The Berry connection between eigenstates $i\langle u_{m\mathbf{q}} | \partial_{\mathbf{q}} u_{m'\mathbf{q}'} \rangle = [\mathcal{R}]^{mm'}$ and we get $\mathcal{R} = \hat{\phi}(\tau_0 - \frac{\Delta}{E_q} \tau_z - \frac{v_F}{2E_q} \tau_x) - \hat{\mathbf{q}}(\frac{\Delta v_F}{2E_q^2}) \tau_y$ with $\hat{\mathbf{q}} = \cos \phi \hat{\mathbf{x}} + \sin \phi \hat{\mathbf{y}}$ and $\hat{\phi} = -\sin \phi \hat{\mathbf{x}} + \cos \phi \hat{\mathbf{y}}$.

The symmetrized OAM operator is given by the expression $\hat{\mathbf{L}} = \frac{m_0}{4}(\hat{\mathbf{r}} \times \hat{\mathbf{v}} - \hat{\mathbf{v}} \times \hat{\mathbf{r}})$ where $m_0 = -\hbar/(g_L \mu_B)$ with g-factor $g_L = 1$ and Bohr-magneton $\mu_B = \frac{e\hbar}{2m_e}$, while $\hat{\mathbf{r}}$ and $\hat{\mathbf{v}}$ represent the position and velocity operators respectively. In the Bloch eigenstate basis, the position operator and velocity operator can be expressed in terms of Berry connection. The position operator can be written as $[\hat{\mathbf{r}}]_{\mathbf{q}\mathbf{q}'}^{mm'} = i \frac{\partial \delta(\mathbf{q}-\mathbf{q}')}{\partial \mathbf{q}} \delta_{m,m'} + [\mathcal{R}]^{mm'} \delta(\mathbf{q}-\mathbf{q}')$ and the velocity operator is $[\hat{\mathbf{v}}]_{\mathbf{q}\mathbf{q}'}^{mm'} = [\frac{i}{\hbar} [H_0, \hat{\mathbf{r}}]]_{\mathbf{q}\mathbf{q}'}^{mm'} = \frac{1}{\hbar} \frac{\partial E_{\mathbf{q}}^m}{\partial \mathbf{q}} \delta_{m,m'} + \frac{i}{\hbar} (E_{\mathbf{q}}^m - E_{\mathbf{q}'}^{m'}) [\mathcal{R}]^{mm'}$. Only the z -component of OAM for graphene or TMDs model survives, $L_z = -(\hbar/g_L \mu_B)(v_F^2 \Delta/2\hbar E_q^2) \tau_0$ [33].

The expectation value of the OH-current is calculated by taking trace of $\mathbf{j} = \text{Tr}[\hat{\rho} \hat{\mathbf{j}}]$. When the electric field is applied along $\hat{\mathbf{x}}$, the transverse orbital Hall current is $\parallel \hat{\mathbf{y}}$ with $j_y^z = \text{Tr}[\rho_E^{(0)} \hat{j}_y^z]$, where $\hat{j}_y^z = 1/2\{L_z, \hat{v}_y\}$ and Tr represents the full operator trace. One finds the density matrix ρ_E up to zero order of the impurity density $\rho_E = n_E^{(-1)} + S_E^{(0)} + n_E^{(0)}$, where $n_E^{(-1)}$ is diagonal part of the density matrix to leading order in the impurity density, $S_E^{(0)}$ is off-diagonal part of the density matrix from intrinsic off-diagonal driving term and anomalous driving term depending on disorder [54], and $n_E^{(0)}$ is diagonal part of the density matrix to next-to-leading order in the impurity density. Off-diagonal part of the density matrix $S_E^{(0)}$ has two sources: intrinsic driving term $D_{E\mathbf{q}}^{mm'} = \frac{eE}{\hbar} \cdot \{i\mathcal{R}^{mm'} [f^{(0)}(E_{\mathbf{q}}^m) - f^{(0)}(E_{\mathbf{q}'}^{m'})]\}$ with $f^{(0)}(E_{\mathbf{q}}^m)$ the

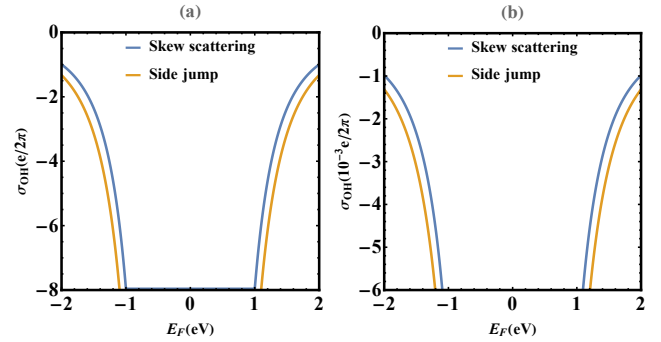


Figure 3. The skew scattering and side jump contributions to OH-conductance σ_{OH} vs the Fermi energy E_F : (a) for the 2H-phase monolayer MoS₂ with the parameters $v_F = 3.6 \text{ eV/Å}$ and $\Delta = 0.883 \text{ eV}$; (b) for the tilted 2D massive Dirac model with $v_F = 1 \text{ eV/Å}$ and $\Delta = 0.1 \text{ eV}$ and $v_t = 0.1 v_F$.

Fermi distribution function in equilibrium, and anomalous driving term $D_{E\mathbf{q}}^{mm'} = -J_{\text{off}}^{mm'} [n_E^{(-1)}(\mathbf{q})]$. The solution of $[S_E^{(0)}]^{mm'} = -i\hbar (D_{E\mathbf{q}}^{mm'} + D_{E\mathbf{q}'}^{mm'})/(E_{\mathbf{q}}^m - E_{\mathbf{q}'}^{m'})$. The solution of $n_E^{(0)}(\mathbf{q})$ can be found by $J_{\text{dia}}^{mm'} [n_E^{(0)}(\mathbf{q})] = -J_{\text{dia}}^{mm'} [S_E^{(0)}(\mathbf{q})] - J_E^{mm'} [\rho^{(0)}(\mathbf{q})]$ [Details in Supplement].

The various contributions to the OHE can be categorized as intrinsic, skew scattering, and side jump, in analogy with the anomalous and spin Hall effects. The intrinsic OHE arises from the driving term $D_{E\mathbf{q}}^{mm'}$, giving

$$\sigma_{\text{OH}}^{\text{int}} = -\frac{g_s g_{\nu}}{4\pi} \frac{e m_e v_F^2}{3\hbar^2 \Delta} \frac{\Delta^3}{(v_F^2 q_F^2 + \Delta^2)^{3/2}}. \quad (6)$$

In our density matrix language, the side jump is further separated into two contributions, and the first part calculated by $\text{Tr}[S_E^{(0)} \hat{j}^z]$ where $S_E^{(0)}$ is the part from anomalous driving term $D_{E\mathbf{q}}^{mm'}$ and it is a Fermi surface contribution. Another side jump contribution arises from the electrical field corrected $J_E(\langle \rho \rangle) = \frac{i}{\hbar} \langle [U, g_E] \rangle$ [57]. The total side jump contribution is

$$\sigma_{\text{OH}}^{\text{sd}} = -12 \frac{g_s g_{\nu}}{6\pi} \frac{e m_e v_F^2}{3\hbar^2 \Delta} \frac{\Delta^3}{(v_F^2 q_F^2 + \Delta^2)^{3/2}}. \quad (7)$$

The skew scattering contribution is determined from the scattering integral $J_{\text{dia}}^{mm'} [S_E^{(0)}(\mathbf{q})]$,

$$\sigma_{\text{OH}}^{\text{sk}} = -9 \frac{g_s g_{\nu}}{4\pi} \frac{e m_e v_F^2}{3\hbar^2 \Delta} \frac{\Delta^3}{(v_F^2 q_F^2 + \Delta^2)^{3/2}}, \quad (8)$$

and it is also a Fermi surface contribution. So the total extrinsic OHE is $\sigma_{\text{OH}}^{\text{ext}} = \sigma_{\text{OH}}^{\text{sd}} + \sigma_{\text{OH}}^{\text{sk}} = 21 \sigma_{\text{OH}}^{\text{int}}$. We plot the individual extrinsic contributions separately in Fig. 3.

Topological antiferromagnets. These are important for orbital torque applications. Since an external electric field can interact directly with orbital degrees of freedom without requiring the spin-orbit interaction, electrical generation of OAM can rely on light atomic elements

[56, 58–60], widening the material choice for the electrical control of magnetism [20, 61, 62]. Since the absence of spin-orbit coupling could result in long-lived magnetic information [5], the orbital torque is investigated as an alternative to the spin torque, which has applications in data storage and nonvolatile logic [4, 63, 64].

Topological antiferromagnets are described by a tilted Dirac Hamiltonian [19]. We can generalize the calculation above to the tilted massive 2D Dirac system, writing the Hamiltonian as

$$H_0(\mathbf{q}) = \nu v_t q_x \tau_0 + v_F (q_x \tau_y - \nu q_y \tau_x) + \Delta \tau_z, \quad (9)$$

where v_t term introduces tilt along q_x -axis, ν is the valley index, v_F is the Fermi velocity, $\tau_{x,y,z}$ are Pauli matrices for the real spin. This Hamiltonian breaks both \mathcal{T} - and \mathcal{P} -symmetry. Take $\nu = 1$, the dispersion for this two band model is given by $E_{\mathbf{q}}^{\pm} = v_t k_x \pm E_q$ where $E_q = \sqrt{v_F^2 q^2 + \Delta^2}$. The tilt will get into the energy conservation function in the scattering integral and Fermi distribution function. The eigenstates of the Hamiltonian are $|u_{+\mathbf{q}}\rangle = (ie^{-i\phi} u_q, v_q)^T$ and $|u_{-\mathbf{q}}\rangle = (ie^{-i\phi} v_q, -u_q)^T$, where the tilt doesn't get into the eigenstates. The Berry connection between eigenstates $i\langle u_{m\mathbf{q}} | \partial_{\mathbf{q}} u_{m'\mathbf{q}} \rangle = [\mathcal{R}]^{mm'}$, and we get $\mathcal{R} = \hat{\phi} \left(\tau_0 + \frac{\Delta}{E_q} \tau_z + \frac{v_F}{2E_q} \tau_x \right) - \hat{\mathbf{q}} \left(\frac{\Delta v_F}{2E_q^2} \right) \tau_y$. Following the calculation in the last section, the z -component of OAM for topological antiferromagnets will have a sign difference because of the Berry connections. To determine the OHE for the tilted 2D massive Dirac system one can expand the tilt up to first order in the energy function by assuming $v_t/v_F \ll 1$. So in the scattering process, the energy conservation function can be expanded as $\delta(E_{\mathbf{q}}^m - E_{\mathbf{q}'}^m) \approx \delta(E_q - E_{q'}) + v_t q (\cos \phi - \cos \phi') \frac{\partial \delta(E_q - E_{q'})}{\partial E_q}$. In a similar manner, the Fermi distribution function in equilibrium and at the absolute zero of temperature can also be expanded, for example, with E_F lying in conduction band one can write $f^{(0)}(E_{\mathbf{q}}^+) \approx \Theta(E_F - E_{\mathbf{q}}^+) = \Theta(E_F - E_q) + v_t q \cos \phi \frac{\partial \Theta(E_F - E_q)}{\partial E_q}$. In this way, one can solve the density matrix up to first order tilt. Then the density matrix can be decomposed as $\rho_E + \rho_{E,v_t}$, where $\rho_E = n_E^{(-1)} + S_E^{(0)} + n_E^{(0)}$ the solution with $v_t = 0$ and $\rho_{E,v_t} = n_{E,v_t}^{(-1)} + S_{E,v_t}^{(0)} + n_{E,v_t}^{(0)}$ is the correction to first order in the tilt. The expansion involves an angular factor, which, in the operator trace, is further multiplied by angular factors in the density matrix and velocity operator. The product of these three angular factors causes the correction to the OHE to first order in the tilt to vanish. Therefore, our calculation of the OHE in the 2D massive Dirac model is applicable to the tilted 2D massive Dirac model as well, up to terms of second order in the tilt. Based on the values in Refs. [65, 66], we expect such terms to account for < 5% of the total.

Discussion. Our transport theory incorporates, on the same footing, both the intrinsic and the extrinsic OHE in a weakly disordered 2D topological material by carefully accounting for all scattering processes present in the

Born approximation. To the best of our knowledge, the extrinsic OHE, including skew-scattering and side-jump, has only been considered theoretically by Bernevig *et al.* in hole-doped Si [32]. The effect of impurities in the Kubo linear response theory of Ref. [32] is twofold: through the vertex correction to the current operator and through the self-energy. The vertex corrections are taken into account within the ladder type and the so-called skew-scattering type. Bernevig *et al.* showed that vertex corrections from impurity scattering vanish for a low-energy model for hole-doped Si. Therefore the OHE for hole-doped Si is robust against disorder [32]. In light of this, we attribute the large extrinsic OHE in graphene and monolayer TMDs systems to their Dirac dispersion [67].

Our results recall the strong role played by disorder in the anomalous Hall effect of Dirac fermions where, when E_F lies in the conduction or valence bands, extrinsic effects overwhelm intrinsic effects by a factor of 7 [55, 57]. Here the extrinsic OHE is 21 times the intrinsic contribution. Recalling that for Dirac fermions the velocity and spin operators coincide, these factors are understandable in light of the qualitative difference between the orbital and spin angular momentum operators [68].

Some words are in order regarding the range of applicability of our theory. Firstly, since most the orbital moment contribution comes from the valley points [69], we have considered the OHE from the K and K' points, without including the contribution from Γ and the remainder of the Brillouin zone. Secondly, the theory requires $E_F \tau / \hbar > 1$, which excludes the low-density regions in the vicinity of the conduction and valence band edges. These regions are virtually impossible to capture by most theoretical approaches. If one assumes a momentum relaxation time $\tau \approx 1$ ps, our theory is valid once E_F is more than ≈ 50 meV away from either band edge.

We have assumed short-range disorder. For a more generic disorder model, although we do not expect the results to change qualitatively, the RHS of Eqs. (7) and (8) will depend on the angular characteristics of the scattering potential. Disorder effects beyond the Born approximation, including disorder correlations, may influence the extrinsic contribution [70–72]. Considering the dominance of scattering processes in doped systems it is natural to expect weak localization to play an important role in the OHE, a matter that requires further investigation.

Conclusions. We have determined the disorder contribution to the OHE of 2D massive Dirac fermions and shown that it exceeds the intrinsic contribution by an order of magnitude, using graphene, transition metal dichalcogenides and topological antiferromagnets as prototypes. The calculation offers an approach to tuning and maximizing the orbital torque and can be extended to other classes of materials, such as Weyl and Dirac semimetals, topological insulators, and van der Waals heterostructures, as well as opening future perspectives on graphene-based orbitronics and twistronics, since magic-angle twisted bilayer graphene is the first material with purely orbital-based magnetism [73].

Acknowledgments. This work is supported by the Australian Research Council Centre of Excellence in Future Low-Energy Electronics Technologies, project number

CE170100039. We acknowledge enlightening discussions with Di Xiao, Giovanni Vignale, Eli Zeldov, Binghai Yan, Amit Agarwal and Kamal Das.

[1] N. Nagaosa, J. Sinova, S. Onoda, A. H. MacDonald, and N. P. Ong, *Rev. Mod. Phys.* **82**, 1539 (2010).

[2] J. Sinova, S. O. Valenzuela, J. Wunderlich, C. H. Back, and T. Jungwirth, *Rev. Mod. Phys.* **87**, 1213 (2015).

[3] A. Johansson, B. Göbel, J. Henk, M. Bibes, and I. Mertig, *Phys. Rev. Res.* **3**, 013275 (2021).

[4] Q. Shao, P. Li, L. Liu, H. Yang, S. Fukami, A. Razavi, H. Wu, K. Wang, F. Freimuth, Y. Mokrousov, M. D. Stiles, S. Emori, A. Hoffmann, J. Åkerman, K. Roy, J.-P. Wang, S.-H. Yang, K. Garello, and W. Zhang, *IEEE Transactions on Magnetics* **57**, 1 (2021).

[5] T. S. Seifert, D. Go, H. Hayashi, R. Rouzegar, F. Freimuth, K. Ando, Y. Mokrousov, and T. Kampfrath, *Nature Nanotechnology* (2023), 10.1038/s41565-023-01470-8.

[6] S. Kobayashi and A. Furusaki, *Phys. Rev. B* **104**, 195114 (2021).

[7] Y.-G. Choi, D. Jo, K.-H. Ko, D. Go, K.-H. Kim, H. G. Park, C. Kim, B.-C. Min, G.-M. Choi, and H.-W. Lee, *Nature* **619**, 52 (2023).

[8] P. Wang, Z. Feng, Y. Yang, D. Zhang, Q. Liu, Z. Xu, Z. Jia, Y. Wu, G. Yu, X. Xu, and Y. Jiang, *npj Quantum Materials* **8**, 28 (2023).

[9] F. Xue, V. Amin, and P. M. Haney, *Phys. Rev. B* **102**, 161103 (2020).

[10] D. Jo, D. Go, and H.-W. Lee, *Phys. Rev. B* **98**, 214405 (2018).

[11] Z. C. Zheng, Q. X. Guo, D. Jo, D. Go, L. H. Wang, H. C. Chen, W. Yin, X. M. Wang, G. H. Yu, W. He, H.-W. Lee, J. Teng, and T. Zhu, *Phys. Rev. Res.* **2**, 013127 (2020).

[12] S. Lee, M.-G. Kang, D. Go, D. Kim, J.-H. Kang, T. Lee, G.-H. Lee, J. Kang, N. J. Lee, Y. Mokrousov, S. Kim, K.-J. Kim, K.-J. Lee, and B.-G. Park, *Communications Physics* **4**, 234 (2021).

[13] Y. Yafet, *Solid State Physics* Eds. Seitz and Turnbull **14**, 1 (1963).

[14] M.-C. Chang and Q. Niu, *Phys. Rev. Lett.* **75**, 1348 (1995).

[15] M.-C. Chang and Q. Niu, *Journal of Physics: Condensed Matter* **20**, 193202 (2008).

[16] M.-C. Chang and Q. Niu, *Phys. Rev. B* **53**, 7010 (1996).

[17] G. Sundaram and Q. Niu, *Phys. Rev. B* **59**, 14915 (1999).

[18] J. N. Fuchs, F. Piéchon, M. O. Goerbig, and G. Montambaux, *The European Physical Journal B* **77**, 351 (2010).

[19] S. Lahiri, T. Bhore, K. Das, and A. Agarwal, *Phys. Rev. B* **105**, 045421 (2022).

[20] J. Kim, D. Go, H. Tsai, D. Jo, K. Kondou, H.-W. Lee, and Y. Otani, *Phys. Rev. B* **103**, L020407 (2021).

[21] J.-P. Hanke, F. Freimuth, S. Blügel, and Y. Mokrousov, *Scientific Reports* **7**, 41078 (2017).

[22] M. Eich, F. c. v. Herman, R. Pisoni, H. Overweg, A. Kurzmann, Y. Lee, P. Rickhaus, K. Watanabe, T. Taniguchi, M. Sigrist, T. Ihn, and K. Ensslin, *Phys. Rev. X* **8**, 031023 (2018).

[23] A. Kurzmann, M. Eich, H. Overweg, M. Mangold, F. Herman, P. Rickhaus, R. Pisoni, Y. Lee, R. Garreis, C. Tong, K. Watanabe, T. Taniguchi, K. Ensslin, and T. Ihn, *Phys. Rev. Lett.* **123**, 026803 (2019).

[24] K. Das, K. Ghorai, D. Culcer, and A. Agarwal, *arXiv*, 2307.12088 (2023).

[25] A. Faridi and R. Asgari, *Phys. Rev. B* **107**, 235417 (2023).

[26] D. Xiao, Y. Yao, Z. Fang, and Q. Niu, *Phys. Rev. Lett.* **97**, 026603 (2006).

[27] T. Yoda, T. Yokoyama, and S. Murakami, *Scientific Reports* **5**, 12024 (2015).

[28] S. Zhong, J. E. Moore, and I. Souza, *Phys. Rev. Lett.* **116**, 077201 (2016).

[29] T. Yoda, T. Yokoyama, and S. Murakami, *Nano Letters* **18**, 916 (2018).

[30] L. Salemi, M. Berritta, A. K. Nandy, and P. M. Oppeneer, *Nature Communications* **10**, 5381 (2019).

[31] S. Ding, Z. Liang, D. Go, C. Yun, M. Xue, Z. Liu, S. Becker, W. Yang, H. Du, C. Wang, Y. Yang, G. Jakob, M. Kläui, Y. Mokrousov, and J. Yang, *Phys. Rev. Lett.* **128**, 067201 (2022).

[32] B. A. Bernevig, T. L. Hughes, and S.-C. Zhang, *Phys. Rev. Lett.* **95**, 066601 (2005).

[33] S. Bhowal and G. Vignale, *Phys. Rev. B* **103**, 195309 (2021).

[34] S. Grover, M. Bocarsly, A. Uri, P. Stepanov, G. Di Battista, I. Roy, J. Xiao, A. Y. Meltzer, Y. Myasoedov, K. Pareek, K. Watanabe, T. Taniguchi, B. Yan, A. Stern, E. Berg, D. K. Efetov, and E. Zeldov, *Nature Physics* **18**, 885 (2022).

[35] L. Salemi and P. M. Oppeneer, *Phys. Rev. B* **106**, 024410 (2022).

[36] D. Go, D. Jo, C. Kim, and H.-W. Lee, *Phys. Rev. Lett.* **121**, 086602 (2018).

[37] H. Kontani, T. Tanaka, D. S. Hirashima, K. Yamada, and J. Inoue, *Phys. Rev. Lett.* **100**, 096601 (2008).

[38] I. Baek and H.-W. Lee, *Phys. Rev. B* **104**, 245204 (2021).

[39] D. Go, D. Jo, H.-W. Lee, M. Kläui, and Y. Mokrousov, *Europhysics Letters* **135**, 37001 (2021).

[40] D. Lee, D. Go, H.-J. Park, W. Jeong, H.-W. Ko, D. Yun, D. Jo, S. Lee, G. Go, J. H. Oh, K.-J. Kim, B.-G. Park, B.-C. Min, H. C. Koo, H.-W. Lee, O. Lee, and K.-J. Lee, *Nature Communications* **12**, 6710 (2021).

[41] S. Ding, A. Ross, D. Go, L. Baldrati, Z. Ren, F. Freimuth, S. Becker, F. Kammerbauer, J. Yang, G. Jakob, Y. Mokrousov, and M. Kläui, *Phys. Rev. Lett.* **125**, 177201 (2020).

[42] D. Go, F. Freimuth, J.-P. Hanke, F. Xue, O. Gomonay, K.-J. Lee, S. Blügel, P. M. Haney, H.-W. Lee, and Y. Mokrousov, *Phys. Rev. Res.* **2**, 033401 (2020).

[43] X. Chen, Y. Liu, G. Yang, H. Shi, C. Hu, M. Li, and H. Zeng, *Nature Communications* **9**, 2569 (2018).

[44] D. Xiao, G.-B. Liu, W. Feng, X. Xu, and W. Yao, *Phys. Rev. Lett.* **108**, 196802 (2012).

[45] T. P. Cysne, S. Bhowal, G. Vignale, and T. G. Rapoport, *Phys. Rev. B* **105**, 195421 (2022).

[46] T. P. Cysne, M. Costa, L. M. Canonico, M. B. Nardelli,

R. B. Muniz, and T. G. Rappoport, Phys. Rev. Lett. **126**, 056601 (2021).

[47] A. Pezo, D. García Ovalle, and A. Manchon, Phys. Rev. B **106**, 104414 (2022).

[48] L. M. Canonico, T. P. Cysne, A. Molina-Sánchez, R. B. Muniz, and T. G. Rappoport, Phys. Rev. B **101**, 161409 (2020).

[49] S. Bhowal and S. Satpathy, Phys. Rev. B **102**, 035409 (2020).

[50] S. Nandy and I. Sodemann, Phys. Rev. B **100**, 195117 (2019).

[51] C. Ortix, Advanced Quantum Technologies **4**, 2100056 (2021).

[52] Z. Z. Du, C. M. Wang, H.-P. Sun, H.-Z. Lu, and X. C. Xie, Nature Communications **12**, 5038 (2021).

[53] Z. Z. Du, H.-Z. Lu, and X. C. Xie, Nature Reviews Physics **3**, 744 (2021).

[54] D. Culcer, A. Sekine, and A. H. MacDonald, Phys. Rev. B **96**, 035106 (2017).

[55] N. A. Siniatsyn, A. H. MacDonald, T. Jungwirth, V. K. Dugaev, and J. Sinova, Phys. Rev. B **75**, 045315 (2007).

[56] H. Kontani, T. Tanaka, D. S. Hirashima, K. Yamada, and J. Inoue, Phys. Rev. Lett. **102**, 016601 (2009).

[57] R. B. Atencia, Q. Niu, and D. Culcer, Phys. Rev. Res. **4**, 013001 (2022).

[58] T. Tanaka, H. Kontani, M. Naito, T. Naito, D. S. Hirashima, K. Yamada, and J. Inoue, Phys. Rev. B **77**, 165117 (2008).

[59] L. Salemi and P. M. Oppeneer, Phys. Rev. Mater. **6**, 095001 (2022).

[60] K. Das and A. Agarwal, Phys. Rev. B **103**, 125432 (2021).

[61] S. Lee, M.-G. Kang, D. Go, D. Kim, J.-H. Kang, T. Lee, G.-H. Lee, J. Kang, N. J. Lee, Y. Mokrousov, S. Kim, K.-J. Kim, K.-J. Lee, and B.-G. Park, Communications Physics **4**, 234 (2021).

[62] D. Hovančík, J. Pospíšil, K. Carva, V. Sechovský, and C. Piamonteze, Nano Letters **23**, 1175 (2023).

[63] A. Manchon, J. Železný, I. M. Miron, T. Jungwirth, J. Sinova, A. Thiaville, K. Garello, and P. Gambardella, Rev. Mod. Phys. **91**, 035004 (2019).

[64] Y. Wang and H. Yang, Accounts of Materials Research, Accounts of Materials Research **3**, 1061 (2022).

[65] C. Wang, Y. Gao, and D. Xiao, Phys. Rev. Lett. **127**, 277201 (2021).

[66] A. G. Linn, P. Hao, K. N. Gordon, D. Narayan, B. S. Berggren, N. Speiser, S. Reimers, R. P. Campion, V. Novák, S. S. Dhesi, T. K. Kim, C. Cacho, L. Šmejkal, T. Jungwirth, J. D. Denlinger, P. Wadley, and D. S. Dessau, npj Quantum Materials **8**, 19 (2023).

[67] S. Tongay, J. Zhou, C. Ataca, K. Lo, T. S. Matthews, J. Li, J. C. Grossman, and J. Wu, Nano Letters, Nano Letters **12**, 5576 (2012).

[68] S. Han, H.-W. Lee, and K.-W. Kim, Phys. Rev. Lett. **128**, 176601 (2022).

[69] S. Bhowal and S. Satpathy, Phys. Rev. B **101**, 121112 (2020).

[70] I. A. Ado, I. A. Dmitriev, P. M. Ostrovsky, and M. Titov, Europhysics Letters **111**, 37004 (2015).

[71] J.-X. Zhang and W. Chen, Phys. Rev. B **107**, 214204 (2023).

[72] I. A. Ado, I. A. Dmitriev, P. M. Ostrovsky, and M. Titov, Phys. Rev. B **96**, 235148 (2017).

[73] E. Y. Andrei and A. H. MacDonald, Nature Materials **19**, 1265 (2020).